Available online at www.sciencedirect.com
ScienceDirect
International Journal of Thermal Sciences 46 (2007) 835–841
International Journal of Thermal Sciences
www.elsevier.com/locate/ijts

# Film evaporation of drops of different shape above a horizontal plate

Guido Bleiker, Eckehard Specht *

*Institute of Fluid Dynamics and Thermodynamics, Otto-von-Guericke-University of Magdeburg, PO Box 4120, 39016 Magdeburg, Germany*

Received 17 October 2002; received in revised form 12 April 2006; accepted 12 April 2006

Available online 22 February 2007

**Abstract**

On a vapor film, floating drops with volumes of several $cm^3$ are disk-like on horizontal plates, while in contrast, drops with volumes smaller than 0.5 $mm^3$ are spherical. Most of the drops have a volume, and thus a form, between these two boundary shapes. The evaporation time of disk-like drops is represented in a dimensionless manner on the basis of well-known analytical solutions, whereby two newly defined characteristic numbers are introduced. For spherical drops an analytical solution is developed. It is shown that with these characteristic numbers the evaporation time of disks as well as of spheres can be described. However, as a result of changed drop geometry, other values for the exponents of the numbers occur. The evaporation times of intermediate drops, which were determined experimentally by ourselves and taken from the literature, can likewise be described by these characteristic numbers. Their exponents change with the volume between the limit values of the two shapes, sphere and disk.


*Keywords:* Film evaporation; Drop; Evaporation time; Spheres; Disk shape; Evaporation force

## 1. Introduction

Investigations into the evaporation of drops on temperature-controlled surfaces date back to the 18th century. In 1759 the physicist J.G. Leidenfrost [1] was the first to describe a phenomenon named after him, but until the second half of this century little consideration was given to the film evaporation of liquid drops. A summary of past investigations is given in a study by Gottfried et al. [2]. The study of drop evaporation was not intensified until the last 40 years when it became more and more important to technical processes.

A great many experimentally based papers focus on the influence of ambient pressure [3,4], the type of liquid [5–7] and surface parameters (roughness, temperature and material) [4,8, 9] on the evaporation time of large single drops. In addition, mathematical models were developed by Gottfried et al. [2], Wachters et al. [10] and Baumeister et al. [11], thus facilitating the calculation of the vapor film thickness and the rate of evaporation. Baumeister et al. [11] suggested a model permitting an exact solution for the vapor flow under drops with a flat bottom. In contrast, Wachters et al. [10] and Gottfried et al. [2] proceed from a Stokes-type plate-parallel flow. Despite all restrictions of the plate-parallel flow, Gottfried et al. [2] applied this simplification to small, spherical drops. Manifold computation models have been developed for specific problems [8,12–14] on the basis of the papers by Gottfried et al. [2], Wachters et al. [10] and Baumeister et al. [11]. However, these papers do not include computation of smaller drops, under consistent consideration of the exact spherical shape.

To calculate the film evaporation of spherical and disk-like drops, it makes sense to use a coordinate system appropriate to the geometry. Sen and Law [22] were the first to develop a solution for the conservation equations in bipolar coordinates for the film evaporation of spherical drops on the basis of the analytical flow field solution as proposed by Stimson and Jefferey [23]. Assuming isothermal conditions on the drop and the plate, they described a solution for the stationary thermal conduction equation. However, they only calculated the evaporation-induced force acting upon the drop, and did not include the source term required for solution. A consistent calculation of the manner in which the spherical drop evaporates is described by Nguyen and Avedisian [19] in numerical terms and by Zhang and Gogos [25] in analytical terms. However, these authors base their calculations on a single-component inert gas environment. Therefore the results obtained by Nguyen and Avedisian [19] and

* Corresponding author.
*E-mail address:* eckehard.specht@vst.uni-magdeburg.de (E. Specht).

1290-0729/$ – see front matter 
doi:10.1016/j.ijthermalsci.2006.04.016

**Nomenclature**

| | | |
|---|---|---|
| $A$ | area | $m^2$ |
| $d$ | diameter | m |
| $F$ | force | N |
| $G_n$ | Legrende polynomial | |
| $g$ | gravity | $m\,s^{-2}$ |
| $\Delta h$ | vaporation enthalpy | $kJ\,kg^{-1}$ |
| $L$ | Laplace constant | m |
| $M$ | mass | kg |
| $\dot{M}$ | mass flow | $kg\,s^{-1}$ |
| $\dot{m}$ | mass flux | $kg\,s^{-1}\,m^{-2}$ |
| $P_n$ | Legrende polynomial | |
| $p$ | pressure | $N\,m^{-2}$ |
| $\dot{Q}$ | heat flow | W |
| $\dot{q}$ | heat flux | $W\,m^{-2}$ |
| $R$ | radius | m |
| $r$ | radial coordinate | m |
| $T$ | temperature | K |
| $t$ | time | s |
| $t_v$ | vaporation time | s |
| $u$ | coordinate | m |
| $V$ | volume | $m^3$ |
| $v$ | velocity | $m\,s^{-1}$ |
| $y$ | bipolar coordinate | m |
| $z$ | bipolar coordinate | m |

*Greek symbols*

| | | |
|---|---|---|
| $\beta_0$ | phase boundary | |
| $\delta$ | vapor film thickness | m |
| $\delta_0$ | minimum film thickness | m |
| $\eta_0$ | dimensionless drop heigth | |
| $\eta_\delta$ | dimensionless film thickness | |
| $\varphi(\eta)$ | dimensionless transformation variable | |
| $\lambda$ | heat conductivity | $W\,m^{-1}\,K^{-1}$ |
| $\mu_v$ | dynamic viscosity | $kg\,m^{-1}\,s^{-1}$ |
| $\mu$ | coordinate | m |
| $\nu$ | viscosity | $m^2\,s^{-1}$ |
| $\sigma$ | surface tension | $N\,m^{-1}$ |
| $\rho$ | density | $kg\,m^{-3}$ |
| $\psi$ | stream function | |
| $\tau$ | dimensionless time | |

*Dimensionless numbers*

| | |
|---|---|
| $Ga$ | Galilei number |
| $Dv$ | drop evaporation number |
| $Re$ | Reynolds number |
| $\tau$ | time |

*Subscripts*

| | |
|---|---|
| L | liquid |
| max | maximal |
| S | saturations state |
| Dr | drop |
| v | vapor |
| W | wall |
| $\delta$ | phase boundary |
| 0 | initial state |
| g | gravity |
| z | vertical |
| r | radial |
| D | disk like |
| s | spherical |

Zhang and Gogos [25] are not applicable to the film evaporation of single drops. Under the conditions of the film evaporation of drops, a vapor cushion prevents any contact with the hot surface under the drop and, hence, the atmosphere under the drop is saturated. Even a model comparison between the models solved for large drops [10,11] and small drops [19,25] is not possible due to the different boundary conditions assumed. Although there are many mathematical models for the film evaporation of drops, no equation has yet been developed for facilitating the calculation of the evaporation time as a function of drop size, plate temperature and material properties.

On a vapor film, floating water drops with volumes greater than 1 $cm^3$ take on a disk-like shape that is illustrated in Fig. 1. For volumes smaller than 0.5 $mm^3$, drops are spherical as shown in Fig. 2. For volumes between these two values, the drop take on geometric shapes which deviate from the above shapes. Since the drop volume decreases with increasing evaporation time, the initially disk-like drops change to the spherical shape during evaporation. For the investigation of the evaporation time of drops with different shapes, the evaporation process is observed prior to any consideration of the two basic shapes, disk and sphere. In particular, the evaporation time will be described dimensionless for general discussion.

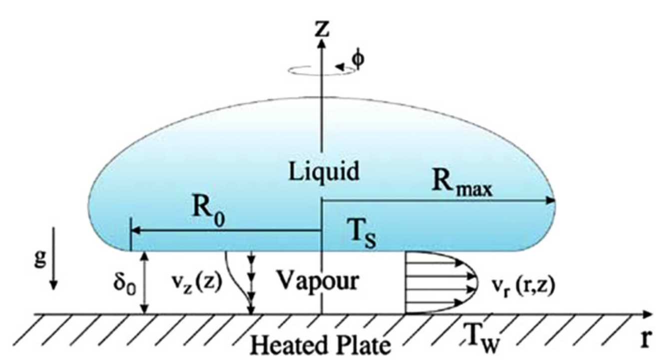


Fig. 1. Large drop (disc-like).

## 2. Disk-like drops

For disc-like drops, the temporal decrease of the mass $M$ can be described as quasi-stationary,

$$\frac{dM}{dt} = -A_0\dot{m}_v \tag{1}$$

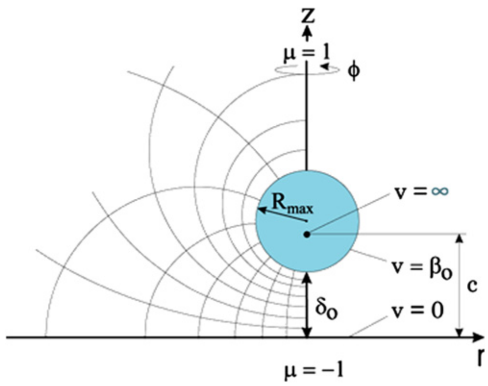


Fig. 2. Small drop (spherical).

Here $A_0 = \pi R_0^2$ is the flat surface of the bottom according to Fig. 1 and $\dot{m}_\mathrm{v}$ the evaporating mass flux. The surface can be replaced in dependence of the drop volume $V_\mathrm{Dr}$ by the Laplace constant [26]

$$A_0 \approx \frac{1}{1.8L} V_\mathrm{Dr} \tag{2}$$

with

$$L = \left( \frac{\sigma}{(\rho_\mathrm{L} - \rho_\mathrm{v}) g} \right)^{1/2} \tag{3}$$

For the drop thickness it thus follows $h = 1.8L$.

The evaporation can be regarded as quasi-stationary, since the mass of the steam below the drop is substantially smaller than that of the liquid. The evaporating mass flux is determined from the condition that the heat flow conducted through the steam film is converted completely into vaporation enthalpy

$$\dot{m}_\mathrm{V} \Delta h = \frac{\lambda_\mathrm{V}}{\delta_0} (T_\mathrm{w} - T_\mathrm{s}) \tag{4}$$

The evaporation on the top surface of the disk and the radiant heat is negligible [19,25]. On the heating plate and at the phase boundary, the wall ($T_\mathrm{w}$) and/or the boiling temperature ($T_\mathrm{s}$) is assumed as constant. The distance of the drop to the wall results from the force equilibrium between the evaporation-induced force below the drop $F_\mathrm{v}$ and the force due to the weight, $F_\mathrm{g}$. For this force is valid

$$F_\mathrm{g} = V_\mathrm{Dr} \rho_\mathrm{L} g \tag{5}$$

The velocity component in the direction of gravity $v_\mathrm{z}$ causes an increased pressure below the drop and thus an upward force. For the computation of this evaporation-induced force the velocity $v_\mathrm{z}$ is needed. This results from the solution of the Navier–Stockes differential equation. For the solution of this equation some simplifications are necessary, the validity of which is proven in [2,10,11,15,18,27]. Thus, for example, the force of inertia of the diverting vapor is neglected. The description of the solution is not explained here but is referred to in Gottfried and Bell [15]. Therefore one reaches the following:

$$F_\mathrm{v} = \frac{3\pi}{2} \nu_\mathrm{v} \frac{R_\mathrm{max}^4}{\delta_0^3} \dot{m}_\mathrm{v} \tag{6}$$

From the above equations it follows for the evaporation time with the assumption $R_\mathrm{max} = R_0$.

$$t_\mathrm{vD} = 4 \left( \frac{3 \cdot 1.8^2 \rho_\mathrm{L}^3 \Delta h^3 L^2 \nu_\mathrm{v}}{2\pi \lambda_\mathrm{v}^3 (T_\mathrm{W} - T_\mathrm{S})^3 g} \right)^{1/4} V_\mathrm{Dr0}^{1/4} \tag{7}$$

Introducing a dimensionless time by including the diameter $d = 2R$

$$\tau = \frac{t_\mathrm{v} \nu_\mathrm{v}}{d^2} \tag{8}$$

the Galilei number

$$Ga = \frac{g d^3}{\nu_\mathrm{v}^2} \tag{9}$$

and the dimensionless number

$$Dv = \frac{\nu_\mathrm{v} \rho_\mathrm{L} \Delta h}{\lambda_\mathrm{v} (T_\mathrm{W} - T_\mathrm{S})} \tag{10}$$

we obtain Eq. (7) in a dimensionless form

$$t_\mathrm{vD} = 4 \left( \frac{3}{8} \right)^{1/4} Dv^{3/4} \left( \frac{1}{Ga} \right)^{1/4} \left( \frac{1.8 \cdot L}{d_0} \right)^{3/4} \tag{11}$$

The geometry ratio $1.8L/d$ corresponds to the ratio height to diameter according to Eq. (2). The dimensionless time is defined in a similar manner to the Fourier number and to the Fick number, in which the thermal diffusity or the diffusity is contained instead of the viscosity. Since this number has not been presented in the literature yet, it is called the dimensionless evaporation time in the following. The characteristic number $D_\mathrm{v}$ is likewise presented here for the first time. In the following it is called drop evaporation number. This characteristic number can be interpreted as a kind of Reynolds number. If one defines a Reynolds number for the drop

$$Re = \frac{v_\mathrm{r}(r = R_0) \delta_0}{\nu_\mathrm{v}} \tag{12}$$

($v_\mathrm{r}$ ($r = R_0$) is, according to Fig. 1, the maximum velocity of the diverted steam), then for the dimensionless evaporation time it follows

$$t_\mathrm{vD} = \left( \frac{1}{2} \right)^{3/4} \frac{1}{Re} \frac{1.8L}{d} \frac{\rho_\mathrm{L}}{\rho_\mathrm{v}} \tag{13}$$

The drop evaporation number and the Galilei number can thus be replaced by the Reynolds number.

With these dimensionless numbers, an analogy between the evaporation of disk-like and spherical drops can now be given. In the following, the computation of the evaporation time of spherical drops is described briefly.

## 3. Spherical drops

For the calculation of the evaporation time the temperature and the velocity field around the spherical drop are needed. These are represented in bipolar coordinates according to Fig. 2.

### 3.1. Temperature field

On the basis of the simplifications valid for the disk-like drop, the heat conduction through the vapor is described by means of the Laplace equation

$$\nabla^2 T = 0 \tag{14}$$

The solution of this equation can be expressed for the interval $-1 \leqslant \mu \leqslant 1$, $0 \leqslant y \leqslant \infty$ after transformation to the new variables of the bipolar coordinate system [17] by means of a separation approach in the form of a Legendre series as follows

$$T = \left(\cosh(y) - \mu\right)^{1/2} \sum_{n=0}^{\infty} G_n(y) P_n(\mu) \tag{15}$$

where

$$G_n(y) = \sqrt{2}\left(k_n \cosh\left(\left(n + \frac{1}{2}\right)y\right) + c_n \sinh\left(\left(n + \frac{1}{2}\right)y\right)\right) \tag{16}$$

and $P_n(\mu)$ is the $n$th Legendre polynomial in the interval $-1 \leqslant \mu \leqslant 1$. The constants $k_n$ and $c_n$ are determined from the boundary conditions on the plate and at the phase boundary. At the phase boundary, $y = \beta_0$, saturation temperature ($T_S$) is assumed.

Along the coordinate $v = 0$, a new boundary condition is assumed here in this study. In the previous studies [19,25], the temperature along the wall ($v = 0$) is assumed to be constant. However, the coordinates $v = 0$ close around the drop at a large distance, so that it is surrounded by the wall in all directions. In order to be able to set the ambient temperature above the drop, in this study the temperature function

$$T(y = 0, \mu) = \varphi(\mu) = T_W - (T_W - T_U)\left(\frac{1 + \mu}{2}\right)^p \tag{17}$$

is assumed as the boundary condition along the coordinate $v = 0$. For the coordinate $\mu = -1$, i.e. under the drop, a constant temperature is thus set, which decreases in the infinite ($v = 0$, $\mu = 1$) to ambient temperature. The exponent $p$ of the function suggested in Eq. (17) indicates the range of the constant heating surface temperature.

By inserting the calculated constants $c_n$ and $k_n$ in the equation, we obtain the temperature distributions around the drop as shown in Fig. 3 for the plate temperature of 400 °C. The figure clearly depicts the constant plate temperature under the drop specified by the boundary condition. The isothermal curves show that the temperature reaches values above the saturation temperature level.

After an insteady heating-up phase, the drop evaporates at saturation temperature across the overall drop surface.

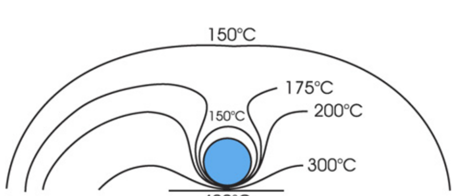


Fig. 3. Calculated temperature field around a water drop.

### 3.2. Flow pattern

For calculating the flow pattern, it is assumed that the flow is quasi stationary and the force of inertia is negligible as was the case for the disk-like drop. The conservation of momentum for the flow pattern can be described by means of the stream function

$$E^4\left(\psi(y, \mu)\right) = 0 \tag{18}$$

$$E^2 = \frac{(\cosh(y) - \mu)}{c^2}\left(\frac{\partial}{\partial y}\left(\left(\cosh(y) - \mu\right)\frac{\partial}{\partial y}\right) + \left(1 - \mu^2\right)\frac{\partial}{\partial u}\left(\left(\cosh(y) - \mu\right)\frac{\partial}{\partial u}\right)\right) \tag{19}$$

as proposed by Stimpson and Jeffery [23]. The solution of the equation is expressed as a series of Gegenbauer polynomials in the form

$$\psi(y, \mu) = \left(\cosh(y) - \mu\right)^{-3/2} \sum_{n=-1}^{\infty} F_n(y) C_{n+1}^{-1/2}(\mu) \tag{20}$$

$$F_n(y) = a_n \cosh\left(\left(n - \frac{1}{2}\right)y\right) + b_n \sinh\left(\left(n - \frac{1}{2}\right)y\right) + c_n \cosh\left(\left(n + \frac{3}{2}\right)y\right) + d_n \sinh\left(\left(n + \frac{3}{2}\right)y\right) \tag{21}$$

$C_{n+1}^{-1/2}(\mu)$ are Gegenbauer polynomials of the order $n + 1$ and the degree $-1/2$. Unlike the solution of these equations as suggested by Stimpson and Jeffery [23], the series solution of the stream function for the case of an evaporation-induced flow starts with $n = -1$ [20]. The integration constants $a_n$, $b_n$, $c_n$ and $d_n$ are determined from the boundary conditions on the plate ($y = 0$)

$$\psi(y = 0, \mu) = 0 \tag{22}$$

$$\left.\frac{\partial \psi}{\partial y}\right|_{y=0} = 0 \tag{23}$$

and at the phase boundary ($y = \beta_0$)

$$\left.\frac{\partial \psi}{\partial y}\right|_{y=\beta_0} = 0 \tag{24}$$

$$\left.\frac{\partial T}{\partial y}\right|_{y=\beta_0} = -\frac{\rho_v \Delta h}{\lambda_v}\frac{(\cosh(\beta_0) - \mu)}{c}\left.\frac{\partial \psi}{\partial \mu}\right|_{v=\beta_0} \tag{25}$$

The calculation of the constants ($a_n, b_n, c_n, d_n$) is not described here as it is mainly based on the paper of Zhang and Gogos [25].

### 3.3. Force equilibrium

The force acting upon the drop because of evaporation can be calculated as proposed by Stimson and Jeffery [23] in bipolar coordinates

$$F_v = \frac{8\sqrt{2}\pi \mu_v}{c} \sum_{n=0}^{\infty} \frac{1}{2n + 3} b_n \tag{26}$$

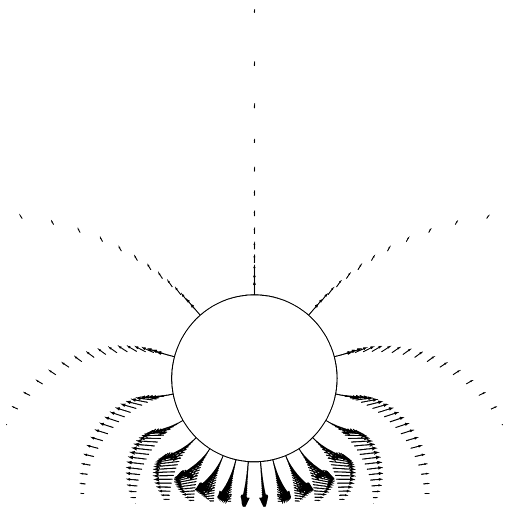

Fig. 4. Velocity field around the drop.

taking account of the new summation basis ($n = -1$). The force of gravity is given by Eq. (5) with $V_{\mathrm{Dr}} = 4/3\pi R^3$. The steam film thickness $\delta_0$ results from the equilibrium of these two forces. Thus the drop distance $\delta_0$ has to be determined iteratively.

### 3.4. Velocity field

In bi-polar coordinates, the velocity components are related to the stream function through the following correlation:

$$v_{\mathrm{v}} = -\frac{(\cosh(y) - \mu)^2}{c^2}\frac{\partial\psi}{\partial\mu}$$
$$v_{\mathrm{u}} = -\frac{(\cosh(y) - \mu)^2}{c^2 \sin(u)}\frac{\partial\psi}{\partial y} \tag{27}$$

The velocity and the temperature field is coupled with Eq. (25). The velocity field around the drop are shown in Fig. 4 under the conditions of Fig. 3. It can be seen that the drop evaporates across the overall drop surface in accordance with the temperature distribution calculated before. With the velocity component nominal to the surface now known it is possible to calculate the total mass flux.

### 3.5. Evaporation time of spherical drops

For the evaporation time of the drop, $t_{\mathrm{v}}$, it follows

$$\int_0^{t_{\mathrm{v}}} \dot{M}_{\mathrm{v}}\,\mathrm{d}t = M_{\mathrm{Dr0}} \tag{28}$$

where $M_{\mathrm{Dr0}}$ is the initial mass of the drop. The corresponding evaporating mass flow is obtained by integrating the phase boundary velocity ($v(\beta_0, \mu)$) across the drop surface

$$\dot{M}_{\mathrm{v}} = -2\pi\rho_{\mathrm{v}} \int_{-1}^{1} h_2^2 v(\beta_0, \mu)\,\mathrm{d}\mu \tag{29}$$

With the film thickness, $\delta_0$, the mass flow is a function of time. Hence, the evaporation time is calculated iteratively. In Fig. 5,

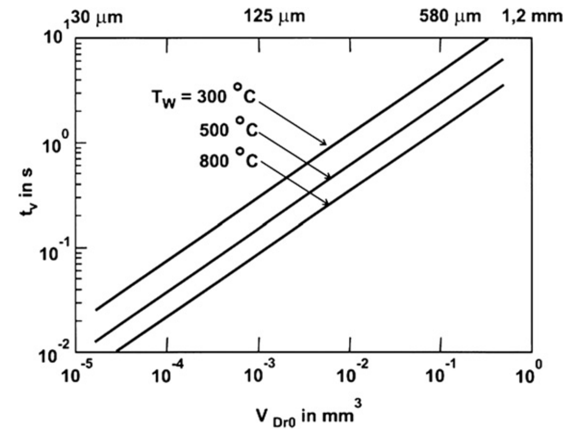


Fig. 5. Evaporation time of spherical drops for three plate temperatures.

the calculated evaporation times are depicted as functions of the initial volume for three plate temperatures.

A parameter variation was performed to investigate the analogy of the behaviour of material properties. It turned out that the material property factor $\rho_{\mathrm{L}}\Delta h/\lambda_{\mathrm{v}}$ appears in the same combination as for the disk-like drop, however, in the case with a higher power of 1 instead of 3/4. The gravitational acceleration ($g$) and the viscosity ($\nu_{\mathrm{v}}$) also exert only a very little influence. Hence, the equation

$$t_{\mathrm{vs}} = 0.108\frac{\rho_{\mathrm{L}}\Delta h}{\lambda_{\mathrm{v}}(T_{\mathrm{W}} - T_{\mathrm{S}})}\left(\frac{\nu_{\mathrm{v}}^2}{g}\right)^{1/15} V_{\mathrm{Dr0}}^{3/5} \tag{30}$$

is well suited to approximate the evaporation time of spherical drops with a deviation of $\pm 1.5\%$ as indicated by means of the solid line in Fig. 5. Using the dimensionless parameter according to Eqs. (9) and (10) we obtain the dimensionless evaporation time of the spherical drop

$$t_{\mathrm{vs}} = 0.108\left(\frac{\pi}{6}\right)^{3/5} Dv\left(\frac{1}{Ga}\right)^{1/15} \tag{31}$$

As can be seen, the dimensionless evaporation time of the spherical drop is described with the same parameters as the dimensionless evaporation time of the disk-like drop. Only the drop diameter-to-height ratio is excluded in this equation because for a spherical drop this ratio is one. Only the exponents of both parameters are different for spherical and disk-like drops.

## 4. Evaporation time for intermediate shapes

As mentioned at the beginning, the shape of the drop depends on its volume. The water drop is spherical at volumes smaller than $5 \times 10^{-1}$ mm$^3$ which corresponds to a diameter below 1 mm. In contrast, the drop is disk-like when its volume is larger than about $8 \times 10^4$ mm$^3$ which corresponds to a disk diameter of about 26 mm. The evaporation time depends on the volume of spherical drops to the power of 3/5 and of disk-like drops to the power of 1/4. Hence, the influence of the volume on the evaporation time changes for intermediate shapes between the two boundary cases of spherical and disk-like drops. The evaporation times of drops with such intermediate shapes

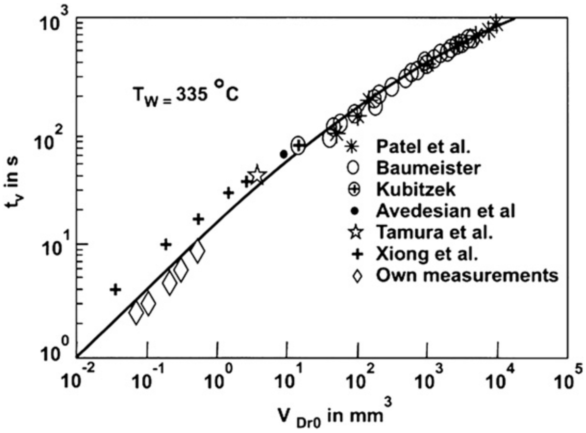


Fig. 6. Comparison between evaporation times obtained experimentally and calculated values at a plate temperature of $T_W = 335\ ^{\circ}C$.

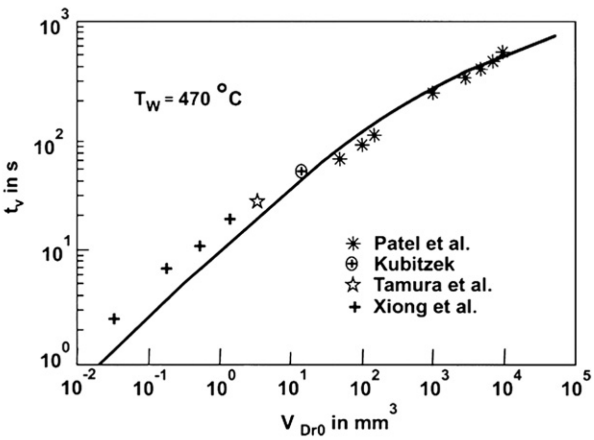


Fig. 7. Comparison between evaporation times obtained experimentally and calculated values at a plate temperature of $T_W = 470\ ^{\circ}C$.

can be approximated using the two boundary cases with the following equation

$$t_v = \left( \left( \frac{1}{t_{vs}} \right)^{1.6} + \left( \frac{1}{t_{vD}} \right)^{1.6} \right)^{-1/1.6} \tag{32}$$

as a result of data fitting. Figs. 6 and 7 depict the evaporation time of water drops on plates with temperatures, for example, of $335\ ^{\circ}C$ and $470\ ^{\circ}C$ as a function of volume in a double logarithmic scale. For volumes smaller than $5 \times 10^{-1}\ mm^3$ the approximation curve, according to the equation above, changes into a straight line exhibiting a $3/5$ gradient, whereas the straight line exhibits a $1/4$ gradient at volumes higher than $8 \times 10^4\ mm^3$. In addition, Fig. 6 contains evaporation times established by various authors. However, none of the authors has yet obtained results from experimental investigations describing the overall shape range of the single drop from a spherical up to a disk-like shape. Whereas the overwhelming number of experimental studies [7,9,11,21,26] deals with large liquid drops, studies by Xiong [24] focus on the evaporation of small spherical liquid drops.

Therefore we carried out our own measurements particularly for small volumes. For this we used Kubitzek's [16] experimental set up, in order to be able to extend the range from large to small drops under the same experimental conditions. Using a special mechanism to prevent vibration, the drops were placed on a heated plate of constant temperature. The evaporation of the drop was observed with a high-velocity camera. For the detailed description of the experiments please refer to Kubitzek [16] and Bleiker [27].

The influence of the drop shape on the evaporation time becomes clear on the basis of a comparison of the evaporation times indicated by several authors for different droplet sizes. As can be seen in Fig. 6 the increasing rate with decreasing drop volume deduced from the theoretical models is confirmed by the experimental measurements. Also in the case of the higher plate temperature of $470\ ^{\circ}C$ (Fig. 7), the calculated and the experimentally established evaporation times correspond well, as could be seen in Fig. 6.

## 5. Conclusions

- The most drops, evaporating on a horizontal flat hot surface, have shapes between the two limiting shapes of a sphere (very small drops) and of a disk (greater drops). It is shown that the evaporation time of these intermediate drop shapes can be approximated well using the evaporation times of spherical and disk-like drops (Eq. (32)).
- The evaporization time of disk-shaped drops can be described with a dimensionless equation. Therefore, the analytical models presented in the literature were transformed into dimensionless groups. Two new dimensionless parameters had to be introduced, the dimensionless time (Eq. (8)) and a so called drop evaporation number (Eq. (10)). The dimensionless time is defined similar to the Fourier- and Ficknumber, however, with the viscosity instead of the diffusities. The evaporation number includes the latent heat of vaporation and the drifting temperature difference between wall and drop.
- The evaporation time of spherical drops can be calculated using the same dimensionless parameters. To proof this, an analytical model presented in the literature had to be transformed. This model had been extended using a new boundary layer for the temperature profile. Herewith it is shown, that the evaporation takes place around the total surface and not only on the bottom surface.
- Using the dimensionless parameters the evaporation time of the droplets can be calculated relative easily with an exponential formulation. The equations given in other studies have to be solved iteratively on basis of an infinite series of Legendre and Gegenbauer polynomials.
- The calculated times match with own measured values and those presented in the literature. With our model and equations, especially the influence of the wall temperature and of the drop volume and therewith the shape of the drop can be described in a clear manner.

## References

[1] J.G. Leidenfrost, De Aquae Communis Nonnullis Qualitatibus Tractatus, Duisburg 1759. Translation: On the fixation of water in diverse fire, Int. J. Heat Mass Transfer 9 (1966) 1153–1166.

[2] B.S. Gottfried, C.J. Lee, K.J. Bell, The Leidenfrost Phenomenon: film boiling of liquid droplets on a flat plate, Int. J. Heat Mass Transfer 9 (1966) 1167–1187.

[3] G.S. Emmerson, The effect of pressure and surface material on Leidenfrost point of discrete drops of water, Int. J. Heat Mass Transfer 18 (1975) 381–386.

[4] G.S. Emmerson, C.W. Snoek, The effect of pressure on the Leidenfrost point of discrete drops of water and freon on a brass surface, Int. J. Heat Mass Transfer 21 (1978) 1081–1086.

[5] C.T. Avedisian, M. Fatehi, An experimental study of Leidenfrost evaporation characteristics of emulsified liquid droplets, Int. J. Heat Mass Transfer 31 (1988) 1588–1603.

[6] K.J. Baumeister, G.J. Schoessow, C.E. Chmielewski, Film boiling of mercury droplets, Can. J. Chem. Engrg. 55 (1977) 521–526.

[7] Z. Tamura, Y. Tanasawa, Evaporation and combustion of a drop contacting with a hot surface in: Seventh Symp. (Int.) on Combustion, 1959, pp. 509–522.

[8] C.T. Avedisian, J. Koplik, Leidenfrost boiling of methanol droplets on hot porous/ceramic surface, Int. J. Heat Mass Transfer 30 (1987) 379–393.

[9] I. Michiyoshi, K. Makino, Heat transfer characteristics of evaporation of a liquid droplet on heated surfaces, Int. J. Heat Mass Transfer 21 (1978) 605–613.

[10] L.H. Wachters, H. Bonne, H.J. van Nouthuis, The heat transfer from a hot horizontal plate to sessile water drops in the spheroidal state, Chem. Engrg. Sci. 21 (1966) 923–936.

[11] K.J. Baumeister, T.D. Hamill, F.L. Schwartz, G.J. Schoessow, Film boiling heat transfer to water drops on a flat plate, Chem. Engrg. Progr. Symp. Ser. 62 (62) (1966) 52–61.

[12] C.T. Avedisian, D. Ioffredo, M.J. O'Connors, Film boiling of discrete droplets of mixtures of coal and water on a horizontal brass surface, Chem. Engrg. Sci. 39 (1984) 319–327.

[13] S. Chandra, S.D. Aziz, Leidenfrost evaporation of liquid nitrogen droplets, Trans. ASME J. Heat Transfer 116 (1994) 999–1006.

[14] M. Prat, P. Schmitz, D. Poulikakos, On the effect of surface Roughness on the vapor flow under Leidenfrost levitated droplets, J. Fluids Engrg. 117 (1995) 519–525.

[15] B.S. Gottfried, K.J. Bell, Film boiling of spheroidal droplets, I & EC Fundamentals 5 (1966) 561–568.

[16] A.M. Kubitzek, Experimentelle Untersuchung des Phasenübergangs beim Tropfenaufprall auf heiße Wände. Diss. Universität Göttingen, 1997.

[17] N.N. Lebedev, Special Functions and their Applications, Prentice-Hall, Englewood Cliffs, NJ, 1965.

[18] A. Moriyama, Evaporation rate of a single water droplet on hot solid surface, Trans. ISIJ 14 (1974) 290–295.

[19] T.K. Nguyen, C.T. Avedisian, Numerical solution for film evaporation of a spherical liquid droplet on an isothermal and adiabatic surface, Int. J. Heat Mass Transfer 30 (1987) 1497–1509.

[20] H.N. Oguz, S.S. Sadhal, Growth and collapse of translating compound multiphase drops: analysis of fluid mechanics and heat transfer, J. Fluid Mech. 179 (1987) 105–136.

[21] M.B. Patel, K.J. Bell, The Leidenfrost Phenomenon for extended liquid masses, AIChE Preprint 25, presented at the 8th National Heat Transfer Conference, LA, 1965.

[22] A.K. Sen, C.K. Law, On a slowly evaporating droplet near a hot plate, Int. J. Heat Mass Transfer 27 (1984) 1418–1421.

[23] M. Stimson, G.B. Jeffery, The motion of two spheres in a viscous fluid, Proc. R. Soc. London A 111 (1926) 110–116.

[24] T.Y. Xiong, M.C. Yuen, Evaporation of a liquid droplet on a hot plate, Int. J. Heat Mass Transfer 34 (1991) 1881–1894.

[25] S. Zhang, G. Gogos, Film evaporation of a spherical droplet over a hot surface: fluid mechanics and heat/mass transfer analysis, J. Fluid Mech. 222 (1991) 543–563.

[26] K.J. Baumeister, Heat transfer to water droplets on a flat plate in the film boiling regime, PhD thesis, Univ. Florida, 1964.

[27] G. Bleiker, Filmverdampfung von Einzeltropfen auf heißen Oberflächen, Diss. Universität Magdeburg, Shaker Verlag Aachen, 2000.